Journal of Materials Chemistry C

Accepted Manuscript

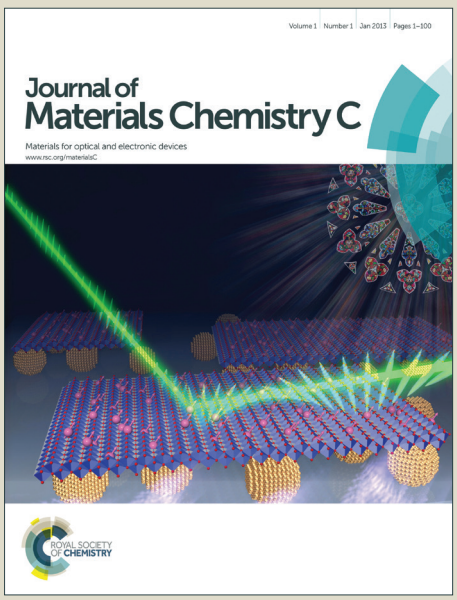

ROYAL SOCIETY OF CHEMISTRY

www.rsc.org/materialsC

Journal Name

RSCPublishing

ARTICLE

Uniform Multi-Nanoparticles Hierarchical Manipulating by Electro-chemical Coupling Assembly

Cite this: DOI: 10.1039/x0xx00000x

Received 00th January 2012,
Accepted 00th January 2012

DOI: 10.1039/x0xx00000x

www.rsc.org/

Jian Zhang,[a,b] Ji Qi,[a] Shusen Kang,[a] Haizhu Sun,[*,b] Mao Li[*,a]

Assembling multiple nanomaterials into a single nanostructure is a promising way to obtain multifucntionality derived from each building block. We address here the need for a general all-solution processed strategy to control the fabrication of multiple nanoparticles (NPs) at room temperature and vacuum free condition. The monodisperse multiple NPs are integrated successively into a thin bulk-hybrid gradient or periodic tandem multilayer films through tuning cycling number of cyclic voltammetry (CV), which base on the quantitatively electrochemical deposition of each kind of NPs thanks to the electrochemical coupling reaction of N-alkylcarbazole ligand. This simple method yields nanoporous, transparent, stable and photoactive films with hierarchical structure of multiple uniform NPs, exemplified by the prototype photodetector devices. Significantly, this strategy opens an avenue to fabricate low-cost, wire, and 3-dimensional NPs films on physically flexible conducting substrates.

Introduction

A large variety of nanoparticles (NPs) play indispensable role as "building blocks" for a variety of materials with superior transport and optical properties for optoelectronics,[1] catalysis,[2] and bio-related applications.[3] Over the last few decades, there has been a huge interest in manipulating tailored NPs building blocks into thin films for optimizing properties of materials with controllable composition, structure, and enhanced performance. Thus, significant efforts have been made over the years to develop bottom-up approaches to tailor film properties in an effective way. The fabrication of nanostructured functional NPs through bottom-up surface modification method[4,5] has been widely used by scientific and engineering communities. For example, organic material has been used to assist and disperse inorganic NPs for fabrication of hybrid film with enhanced performance.[6] However, many issues still remain challenging, such as: (1) fabrication of uniform NPs film, (2) controlling the well-dispersed placement of multi-NPs within thin film, and (3) improving light absorption capabilities of NPs film. Film fabrication of multiple NPs would be ideal to guarantee the sufficient absorption of incident light and funnel the energy level efficiently for facilitating charge transport to electrode.[7] However, in situ NPs generation is often not optimal for such multilayer studies because of the uncontrollable growth and aggregation, which makes extreme difficulty in film fabrication of uniform NPs.

Electropolymerization was introduced for nanoparticle film,[8] however, non-quantitative (unlimited) electrochemical reactions usually result in conducting conjugated polymers with an unavoidable highly doped state. In fact, the resulting conjugated polymers and highly doped states are often unnecessary (or disadvantageous) for a wide library of building blocks. Recently, we have developed quantitatively electrochemical coupling reaction of N-alkylcarbazole[9] and electrochemical coupling (ECC) assembly.[10] In this paper, we focus our attention on electrochemically and quantitatively manipulating of uniform multi-NPs. This simple method affords bulk-hybrid film or periodic multilayered nanostructure with tunable absorption for photovoltaic device serve as both photoactive layer and interface modifier. Significantly, this strategy opens an avenue to fabricate low-cost, wire, and 3-dimensional NPs film on physically flexible conducting substrate.

Results and discussion

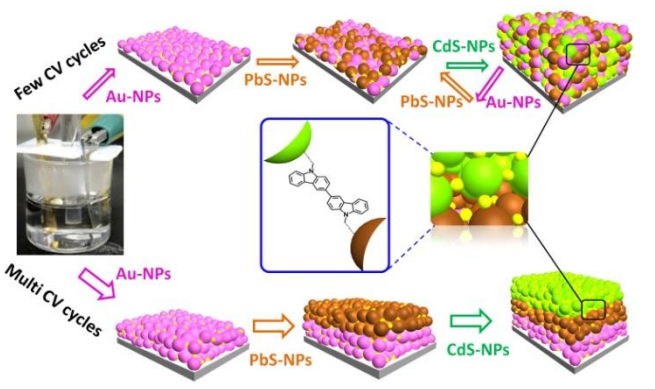

Scheme 1 Manipulating hierarchical composition of NPs Film through controlling successive CV cycles of quantitative electrochemical dimerization of pendent carbazole modified on Au, PbS, and CdS NPs.[12]

The solution processed ECC assembly of inorganic NPs is conducted using <10 nm size NPs (Fig. S1) because of their general interest[11] and favorable diffusion and electromigration to electrode surface. Three typical optical ingredients Au, CdS and PbS NPs capped with peripheral electroactive carbazole units were selected and synthesized. Film assembly of these three kinds of NPs in both homo- and hybrid-mode is successfully conducted through cyclic voltammetry (CV) under open air in solution.

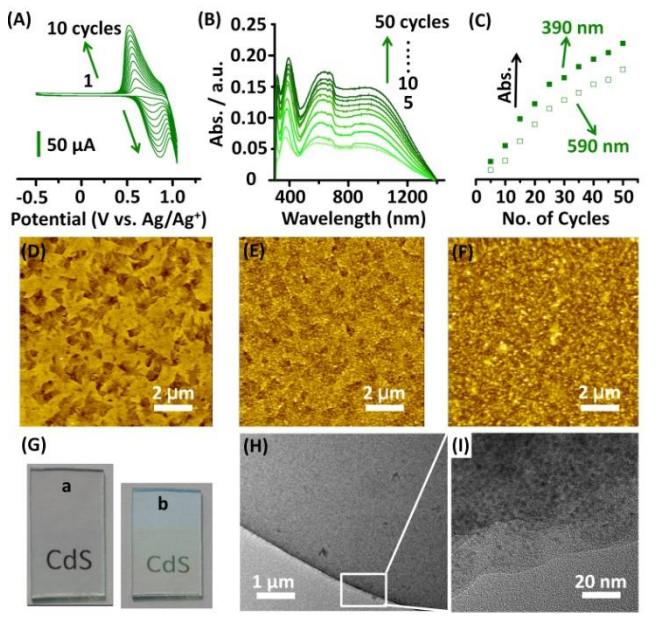

Fig. 1 (A) Successive CV and (B) absorption spectra, (C) peak intensity relationship with CV scan cycles for fabrication of CdS NPs film, and AFM images of ITO surface covered with CdS NPs of 0 (D), 5 (E) and 20 (F) CV scan cycles; (G) Photos of CdS film on ITO (a) without and (b) with sunlight reflection; (H, I) TEM images of CdS NPs film.

As depicted in Scheme 1, ECC assembly of NPs was performed using CV apparatus in order to precisely control over the each single NPs layer through tuning CV cycling numbers, which is superb to conventional method especially on single component LbL film fabrication.[13] Specifically, as for CdS NPs assembly, NPs diffuse to indium tin oxide (ITO) electrode surface then the carbazole units modified on NPs surface oxidized to radical-cation beyond 0.8 V (vs. Ag/Ag^+) during successive CV sweeping between -0.5 and 1.05 V at the rate of 200 mV/s in 1 mg/mL CH_2Cl_2 solution (Fig. 1A). Eventually, the coupling of carbazole radical-cation at 3,6-position forming covalent bond spur the NPs to be addressed onto ITO surface as resulting film. On subsequent CV scan cycles, current density of redox peak arise stepwise, indicating the film forming in a layer by layer manner. The consistent assembly of NPs onto electrode surface was also confirmed by sustained growth of light absorption intensity (Fig. 1B), which shows nearly linear increase upon cycle number (Fig. 1C). According to the absorption spectrum of monodisperse CdS NPs in solution (Fig. S2), peaks at 390 nm and 590 nm are suggested to be ascribed to carbazole dimer and CdS NPs first exciton absorption peak.[14] In addition, a broad absorption band at 800-1400 nm appeared, probably because of the dication species of carbazole dimer, which was reported previously.[15] Since the first exciton absorption coefficient of CdS NPs is lower than that of organic ligand, herein its absorption intensity is comparable to those trace dication of carbazole dimer, which could be ignored in the case of electrochemical fabrication of organic film.[16] The absorption at 800-1400 nm can be efficiently depressed in the case of lower positive scan potential (c.a. 0.85 V),[17] whereas the film absorption intensity is relative lower (Fig. S3), suggesting slow film formation. In order to speed up assembly, we selected the potential at 1.05 V. Atomic force microscopy (AFM) was also performed to investigate the scan cycles influence on film morphology. The feature of ITO morphology (Fig. 1D) was partially and completely covered by NPs topical texture after 5 (Fig. 1E) and 20 scan cycles (Fig. 1F). In contrast to other film fabrication process, the electrochemical assembly has the ability of "self-reparation" and products filled up preferentially the lacunas because of relative high current density in these areas.[17] This uniform film with thickness of 150 nm (Fig. S4) is highly transparent (Fig. 1G(a)) and shows metallic luster under sunlight reflection (Fig. 1G(b)). The CdS NPs film did not show fluorescence probably due to a reversed molecular orbital energy order with respect to the carbazole oligomer and CdSe NPs.[8c]

ECC assembly film is very stable against solvent because of the covalent cross-linking construction between NPs, which make it difficult to go through the examination of TEM for observation of inner structure. In order to solve this problem, water soluble PEDOT-PSS was pre-spin-coated on ITO before the electrochemical assembly fabrication, and that makes the resulting film capable of falling off from ITO after a washing step in water. As depicted in Fig. 1H, the whole piece of CdS NPs film was uniform in particle size and closely stacked between NPs. And the details in Fig. 1I clearly showed a NPs layered nanoporous structure. The close stacking distribution of uniform NPs size may suggest that the electrochemical assembly has the selection ability for small size NPs because of easy kinetic diffusion.

The single component PbS NPs film was also fabricated and investigated. Compared to CdS NPs film, the CV curve of PbS NPs shows an extra shoulder reduction current peak at 0.9 V (Fig. 2A), indicating some extent of 2,7-position coupling.[18] In addition, the PbS NPs baring no carbazole units were also found to be electrochemically active with a similar current peak[19], which is likely to be another contribution factor to the extra shoulder peak. As for absorption spectra, the contribution of PbS NPs first exciton absorption peak (Fig. S1) along with the dication absorption of carbazole dimers intensifies the near-infrared absorption band (Fig. 2B). The highly transparent PbS film (~120 nm) also shows metallic luster under sunlight reflection (Fig. 2C).

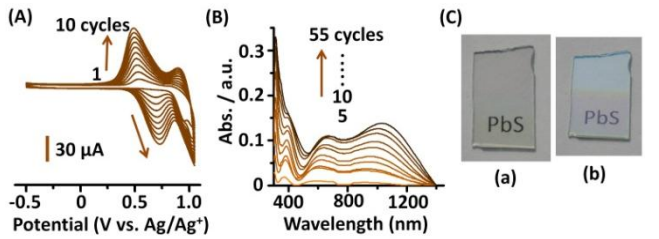

Fig. 2 Successive electrochemical assembly presented in CV (A) and UV-vis spectra (B) of PbS NPs film, and film photos (C) without (a) and with (b) light reflection.

Fabrication of Au NPs film presents similar successive CV curve (Fig. 3A), but different dication absorption feature (Figure 3B) to those of CdS NPs (Fig. 1A, 1B). At the initial stage of electrochemical assembly, thin Au film shows two

main peaks at 382 nm and 560 nm only, which are attributed to carbazole oligomer and plasma effect of Au NPs respectively. As film growing up, a broad absorption band of the carbazole dimer dication emerges and gradually increases along with assembly cycles, probably due to the relatively small amount of carbazyl ligand capped on Au NPs surface compared to those of CdS and PbS NPs, which corresponds well with the smaller current density (Fig. 3A). The highly transparent purple Au film (~320 nm) also shows metallic luster under sunlight reflection (Fig. 3C). The electrochemical assembly NPs film could undergo annealing process to partially remove the surface modified organic ligand of Au NPs. As shown in Fig. 3D, the characteristic absorption peak of Au NPs at 560 nm is significantly enhanced after annealing, as well as Au 4f intensity in XPS spectra, alone with C 1s intensity drops down (Fig. 3E), indicating the elimination of surface organic ligand and that may efficiently enhanced localized surface plasmon resonance (LSPR) of Au NPs. In principle, the nanoporous size of film can be easily controlled by tuning NPs size and shape,[20] which would support their use in applications involving energy storage and conversion,[21] catalytic[22] and various assembly of guest objects.[23]

The hybrid and multilayered film of different NPs are highly desirable because that offers a unique opportunity to flexibly tune the light harvesting upon manipulating the composition and thickness of NPs layers. Thus, an ordered, organized assembly controlled over interface of inter-NPs can be very important. The ECC assembly NPs film is covalently cross-linked, making it very stable for further fabrication of additional layer. Quantitative fabrication of each kind of NPs can realize through tuning CV cycling numbers. In principle, the absorption of NPs film could be tailored to allow maximum overlap with solar spectrum.

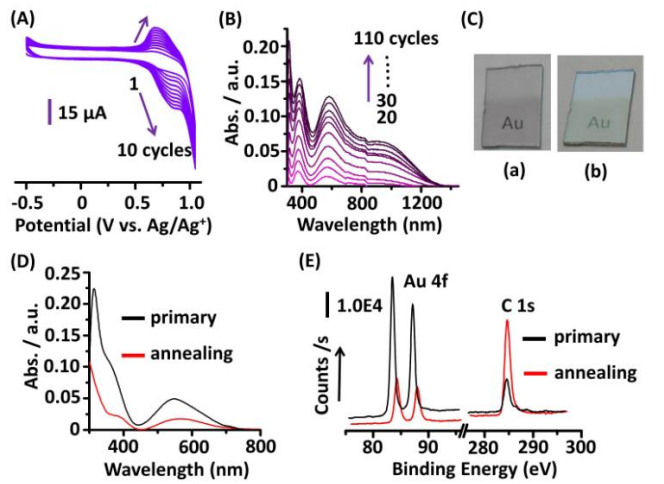

Fig. 3 (A) Successive CV and (B) its corresponding absorption spectra for fabrication of Au NPs film, and (C) film photos (a) without and (b) with light reflection; (D) Absorption and (E) XPS spectra comparison of Au NPs film before and after annealing at 500 ˚C for 1h.

The film growth of Au/PbS NPs hybrid assembly was monitored by absorption spectra. As depicted in Figure 4A, feature absorption peak of Au and PbS NPs presented alternative increase along with stepwise assembly of each component. Resulting film is purplish red in contrast to green metallic luster of ITO (Fig. 4B). AFM images of this film reveal that no phase separation presents on surface and no distinguishable boundaries were found in a cross-section image of SEM (Fig. S5). Therefore, the XPS spectra in vertical etching mode were performed to map the element distribution of Au and PbS hybrid NPs film. As shown in Fig. 4D, the intensity of C1s gradually drops down as etching minutes, indicating a vertical etching process. Meanwhile, the 4f intensity of both Au and Pb show up throughout full process and decrease progressively, demonstrating the Au and PbS NPs are significantly well-mix-located in hybrid film. Comparatively, the XPS spectra of single component Au or PbS NPs film only present their respective Au4f and Pb4f feature peaks (Fig. 4E). Consequently, the multilayer or hybrid film of NPs can be fabricated by controlling cycling number of CV. Frequently alternative electrochemical fabrication of multiple components is favorable for high dispersal in bulk film. The NPs hybrid and multilayer structure are obtained depending on the thickness of every single component layer. In the case of multi CV cycling numbers for thick fabrication of both Au and PbS NPs layers, the resulting film will be a bilayer structure with surface XPS spectra features of single component Au or PbS film. Specifically, as for film structure analysis under multiple CV scan cycles condition, 70 cycles Au NPs film and another additional 50 cycles CdS NPs upon 70 cycles Au film were fabricated. The SEM images show distinguished cross-section morphology between Au film (Fig. 4F) and Au/CdS bilayer film (Fig. 4G). Interestingly, subsequent assembly of CdS layer tend to squeeze the pre-assembly Au to a thinner and more compact layer (Fig. 4G), and the film color totally changes from light purple (Au NPs) to green (CdS NPs), indicating the uniform and even NPs deposition.

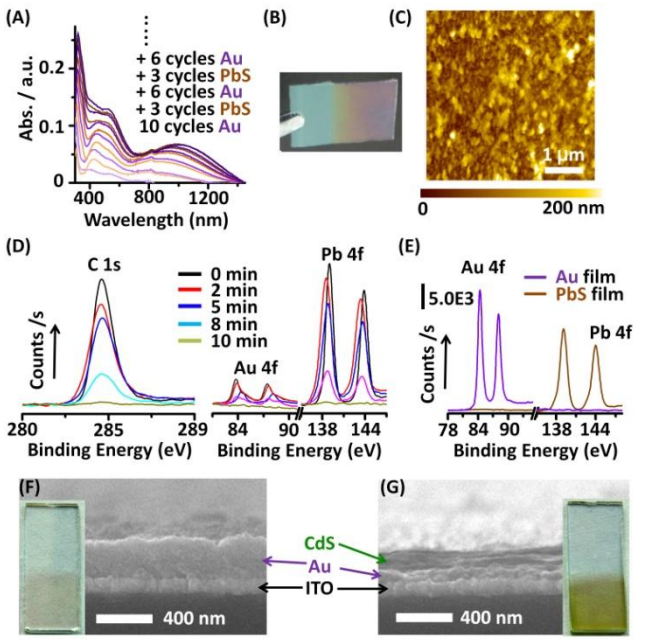

Fig. 4 (A) Absorption spectra of Au/PbS NPs hybrid as-sembly film by alternative electrochemical deposition, and (B) its photo, (C) surface texture, and (D) XPS vertical analysis monitored at etching mode; (E) Single component XPS spectra of Au and PbS NPs film; (F) Photos and cross-section SEM images of (F) Au NPs film and (G) Au/CdS NPs film.

Motivated by these results, transparent, ultrathin, solution processed and closely packed NPs films were applied as photoactive layer and interface modifier in photovoltaic devices. A single layer CdS NPs film was firstly fabricated to photodetector with the prototype structure of ITO/CdS/Al.

Current density-voltage performance was tested upon 430 nm monochromatic light irradiation. As presented in Fig. 5A, the anodic photocurrent increased monotonically with increasing positive bias from -0.5 to 2.0 V, whereas the dark current remained almost constantly low, demonstrating photoconductive behavior of this electrochemical fabricated film. The device EQE can reach 2% in initial tests (Fig. 5B), which is significantly competitive to those of devices fabricated by LbL assembly[24,7b] and spin-coated nanocrystal.[25,26] Meanwhile the device stability is not decent. Specifically, applying under -0.5 V bias, EQE remain almost the same as 0 V, and the EQE curve fluctuates much under more than -1 V bias (Fig. S5). After Au layer was added into device as anode interface layer, photocurrent intensity is slightly decreased (Fig. 5C), meanwhile higher EQE and better device stability is obtained under as high as -3 V bias (Fig. 5D). These devices do not show photovoltaic property beyond 480 nm comparing to the absorption spectra probably due to inefficient dication species of carbazole dimer or ion doped semiconductor NPs. Next, appropriate variation of film structure, composition, and low contact resistance would improve the device performance. For example, the absorption of NPs film could be tailored to allow maximum overlap with solar spectrum. Moreover, electrochemical method was explored as a convenient and cheap way for electrical devices fabrication[16a, 27]. Herein, we further demonstrate its versatility for fabrication films on complex substrates. Electrochemically active fluorescent molecule TCPC which was developed by our group previously was deposited evenly on Pt coil (Fig. 5E) and flexible ITO/PET electrode (Fig. 5F) in high quality. Thus, this electrochemical fabrication is a highly promising strategy to create a new generation of printable dynamic smart systems for 1D wearable,[28] flexible 2D planar platform, and complex 3D substrate, which could lead to large area films fabrication by electrochemical rolling coating with flexible conductive substrates.

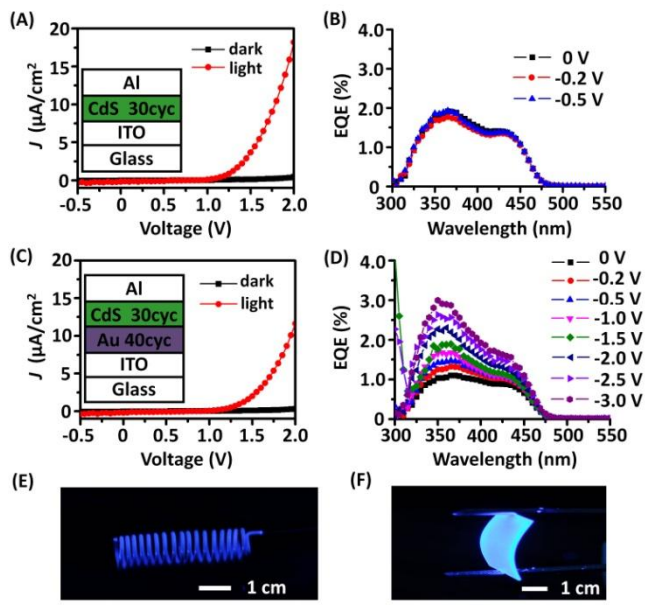

Fig. 5 Photodetector device characterization: (A, C) Current density-voltage profiles upon irradiation of 430 nm monochromatic light with device structure and (B, D) their corresponding EQE characterizations. Photos of fluorescent example electrochemically assembled on (E) 3D Pt wire and (F) flexible ITO/PET electrode.

Conclusions

In summary, we have used the concept of sphere electrochemical packing and demonstrated a well-controlled fabrication strategy to embed multiple CdS, PbS and Au NPs into a bulk-hybrid film. The hierarchical composition of NPs composite film is tunable within gradient or periodic tandem structure, depending on precise quantitative electrochemical fabrication of each component by tuning cycling number applied in CV. This simple process yields nanoporous, transparent, uniform, stable, and photoactive film exemplified by prototypical photodetector device with notable EQE performance. In contrast to conventional methods of LbL assembly for controlling active layer morphology, this approach affords the ability to (a) fabrication film with uniform NPs, (b) pretailor NPs domains with required internal packing and size, (c) obtain stable continuous nanoporous structure, and (d) multiscale control over interface of inter-NPs. Significantly, this electrochemical fabrication method is a highly promising strategy to create a new generation of printable dynamic smart system for 1D wearable, flexible 2D planar platform, and complex 3D substrate, which could achieve large area films fabrication by utilizing roller pulley with flexible conductive substrates.

Acknowledgements

This work was supported by the National Natural Science Foundation of China (21374115) and the Science Technology Program of Jilin Province (201201064 and 20130204025GX), and the Hundred Talents Program, CAS, China.

Notes and references

[a] State Key Laboratory of Polymer Physics and Chemistry, Changchun Institute of Applied Chemistry, Chinese Academy of Sciences, Changchun 130022, P. R. China. E-mail: limao@ciac.ac.cn

[b] College of Chemistry, Northeast Normal University, Changchun 130024, China. E-mail: sunhz335@nenu.edu.cn

† Electronic Supplementary Information (ESI) available: Materials, experimental details, syntheses and characterization of organic ligands and inorganic NPs, additional figures are shown in Supporting Information. See DOI: 10.1039/b000000x/

1 (a) T. Avellini, C. Lincheneau, F. Vera, S. Silvi, A. Credia, *Coord. Chem. Rev.*, 2014, **263-264**, 151-160; (b) W. Song, A. K. Vannucci, B. H. Farnum, A. M. Lapides, M. K. Brennaman, B. Kalanyan, L. Alibabaei, J. J. Concepcion, M. D. Losego, G. N. Parsons, T. J. Meyer, *J. Am. Chem. Soc.*, 2014, **136**, 9773-9779; (c) Q. Liu, Y. Yuan, I. I. Smalyukh, *Nano Lett.*, 2014, **14**, 4071-4077; (d) Y. H. Hu, *Adv. Mater.*, 2014, **26**, 2102-2104.

2 (a) G. Li, Z. Tang, *Nanoscale*, 2014, **6**, 3995-4011; (b) T. Ya-sukawa, H. Miyamura, S. Kobayashi, *Chem. Soc. Rev.*, 2014, **43**, 1450-1461; (c) S. Guo, S. Zhang, S. Sun, *Angew. Chem. Int. Ed.*, 2013, **52**, 8526-8544; (d) M. Zhao, K. Deng, L. He, Y. Liu, G. Li, H. Zhao, Z. Tang, *J. Am. Chem. Soc.*, 2014, **136**, 1738-1741.

3 (a) H. Jans, Q. Huo, *Chem. Soc. Rev.*, 2012, **41**, 2849-2866; (b) K. P. Garc á, K. Zarschler, L. Barbaro, J. A. Barreto, W. O'Malley, L. Spiccia, H. Stephan, B. Graham, *Small*, 2014, **10**, 2516-2529; (c) S. Barua, S. Mitragotri, *Nano Today*, 2014, **9**, 223-243; (d) B. J. Johnson, W. R. Algar, A. P. Malanoski, M. G. Ancona, I. L. Medintz, *Nano Today*, 2014, **9**, 102-131.

4 a) W. Lu, C. M. Lieber, *Nat. Mater.*, 2007, **6**, 841-850; b) R. Shenhar, V. M. Rotello, *Acc. Chem. Res.*, 2003, **36**, 549-561.

5 K. Ariga, J. P. Hill, Q. Ji, *Phys. Chem. Chem. Phys.*, 2007, **9**, 2319-2340.

6 (a) K. C. See, J. P. Feser, C. E. Chen, A. Majumdar, J. J. Urban, R. A. Segalman, *Nano Lett.*, 2010, **10**, 4664-4667; (b) S. Ren, L.-Y. Chang, S.-K. Lim, J. Zhao, M. Smith, N. Zhao, V. Bulović, M. Bawendi, S. Gradečak, *Nano Lett.*, 2011, **11**, 3998-4002; (c) W. Wang, X. Sun, W. Wu, H. Peng, Y. Yu, *Angew. Chem. Int. Ed.*, 2012, **51**, 4644-4647; (d) K. F. Jeltsch, M. Schädel, J.-B. Bonekamp, P. Niyamakom, F. Rauscher, H. W. A. Lademann, I. Dumsch, S. Allard, U. Scherf, K. Meerholz, *Adv. Funct. Mater.*, 2012, **22**, 397-404; (e) P. Hu, Y. Shen, Y. Guan, X. Zhang, Y. Lin, Q. Zhang, C.-W. Nan, *Adv. Funct. Mater.*, 2014, **24**, 3172-3178.

7 (a) T. Franzl, T. A. Klar, S. Schietinger, A. L. Rogach, J. Feldmann, *Nano Lett.*, 2004, **4**, 1599-1603; (b) A. Ruland, C. Schulz-Drost, V. Sgobba, D. M. Guldi, *Adv. Mater.*, 2011, **23**, 4573-4577; (c) E. Talgorn, M. A. de Vries, L. D. A. Siebbeles, A. J. Houtepen, *ACS nano*, 2011, **5**, 3552-3558; (d) D. Gross, A. S. Susha, T. A. Klar, E. Da Como, A. L. Rogach, J. Feldmann, *Nano Lett.*, 2008, **8**, 1482-1485; (e) T. A. Klar, T. Franzl, A. L. Rogach, J. Feldmann, *Adv. Mater.*, 2005, **17**, 769-773; (f) S. Choi, H. Jin, J. Bang, S. Kim, *J. Phys. Chem. Lett.*, 2012, **3**, 3442-3447; (g) H. Jin, S. Choi, H. J. Lee, S. Kim, *J. Phys. Chem. Lett.*, 2013, **4**, 2461-2470; (h) D. Gross, I. Mora-Seró, T. Dittrich, A. Belaidi, C. Mauser, A. J. Houtepen, E. Da Como, A. L. Rogach, J. Feldmann, *J. Am. Chem. Soc.*, 2010, **132**, 5981-5983; (i) H. J. Lee, J. Bang, J. Park, S. Kim, S.-M. Park, *Chem. Mater.*, 2010, **22**, 5636-5643.

8 (a) R. C. Shallcross, G. D. D'Ambruoso, B. D. Korth, H. K. Hall Jr., Z Zheng, J. Pyun, N. R. Armstrong, *J. Am. Chem. Soc.*, 2007, **129**, 11310-11311; (b) H. B. Yildiz, R. Tel-Vered, I. Willner, *Adv. Funct. Mater.*, 2008, **18**, 3497-3505; (c) Y. Park, P. Taranekar, J. Y. Park, A. Baba, T. Fulghum, R. Ponnapati, R. C. Advincula, *Adv. Funct. Mater.*, 2008, **18**, 2071-2078; (d) C. Danda, R. Ponnapati, P. Dutta, P. Taranekar, G. Patterson, R. C. Advincula, *Macromol. Chem. Phys.*, 2011, **212**, 1600-1615; (e) E. Granot, F. Patolsky, I. Willner, J. Phys. Chem. B, 2004, 108, 5875-5881; (f) M. Yamada, H. Nishihara, Langmuir, 2003, 19, 8050-8056.

9 M. Li, S. Ishihara, K. Ohkubo, M. Liao, Q. Ji, C. Gu, Y. Pan, X. Jiang, M. Akada, J. P. Hill, T. Nakanishi, Y. G. Ma, Y. Yamauchi, S. Fukuzumi, K. Ariga, *Small*, 2013, **9**, 2064-2068.

10 M. Li, S. Ishihara, M. Akada, M. Liao, L. Sang, J. P. Hill, V. Krishnan, Y. G. Ma, K. Ariga, *J. Am. Chem. Soc.*, 2011, **133**, 7348-7351.

11 (a) M.-C. Daniel, D. Astruc, *Chem. Rev.*, 2004, **104**, 293-346; (b) A. C. Templeton, W. P. Wuelfing, R. W. Murray, *Acc. Chem. Res.*, 2000, **33**, 27-36.

12 Structures of nanoparticles are shown in ESI.

13 (a) G. K. Such, J. F. Quinn, A. Quinn, E. Tjipto, F. Caruso, *J. Am. Chem. Soc.*, 2006, **128**, 9318-9319; (b) U. Manna, J. Dhar, R. Nayak, S. Patil, *Chem. Commun.*, 2010, **46**, 2250-2252.

14 T. Torimoto, H. Nishiyama, T. Sakata, H. Mori, H. Yoneyama, *J. Electrochem. Soc.*, 1998, **145**, 1964-1968.

15 (a) P. Waenkaew, P. Taranekar, S. Phanichphant, R. C. Advincula, *Macromol. Rapid Commun.*, 2007, **28**, 1522-1527; (b) P. Taranekar, T. Fulghum, A. Baba, D. Patton, R. Advincula, *Langmuir*, 2007, **23**, 908-917; (c) C. Kaewtong, G. Jiang, M. J. Felipe, B. Pulpoka, R. Advincula, *ACS Nano*, 2008, **2**, 1533-1542.

16 (a) M. Li, S. Tang, F. Shen, M. Liu, W. Xie, H. Xia, L. Liu, L. Tian, Z. Xie, P. Lu, M. Hanif, D. Lu, G. Cheng and Y. G. Ma, *Chem. Commun.*, 2006, 3393-3395; (b) M. Li, S. Ishihara, Q. Ji, Y. G. Ma, J. P. Hill, K. Ariga, *Chem. Lett.*, 2012, **41**, 383-385.

17 M. Li, S. Tang, F. Shen, M. Liu, W. Xie, H. Xia, L. Liu, L. Tian, Z. Xie, P. Lu, M. Hanif, D. Lu, G. Cheng, Y. G. Ma, *J. Phys. Chem. B*, 2006, **110**, 17784-17789.

18 (a) A. Iraqi, I. Wataru, *Chem. Mater.*, 2004, **16**, 442-448; (b) P. Taranekar, T. Fulghum, D. Patton, R. Ponnapati, G. Clyde, R. Advincula, *J. Am. Chem. Soc.*, 2007, **129**, 12537-12548.

19 B.-R. Hyun, Y.-W. Zhong, A. C. Bartnik, L. Sun, H. D. Abruña, F. W. Wise,J. D. Goodreau, J. R. Matthews, T. M. Leslie, N. F. Borrelli, *ACS Nano*, 2008, **2**, 2206-2212.

20 J. Watt, S. Cheong, R. D. Tilley, *Nano Today*, 2013, **8**, 198-215.

21 (a) J. Lee, J. Kim, Y. Lee, S. Yoon, S. M. Oh, T. Hyeon, *Chem. Mater.*, 2004, **16**, 3323-3330; (b) J. Pang, V. T. John, D. A. Loy, Z. Yang, Y. Lu, *Adv. Mater.*, 2005, **17**, 704-707; (c) J. Shim, J. Lee, Y. Ye, J. Hwang, S.-K. Kim, T.-H. Lim, U. Wiesner, J. Lee, *ACS Nano*, 2012, **6**, 6870-6881; (d) M. L. Anderson, R. M. Stroud, D. R. Rolison, *Nano Lett.*, 2002, **2**, 235-240; (e) W. Li, Z. Wu, J. Wang, A. A. Elzatahry, D. Zhao, *Chem. Mater.*, 2014, **26**, 287-298; (f) J. Wei, D. Zhou, Z. Sun, Y. Deng, Y. Xia, D. Zhao, *Adv. Funct. Mater.*, 2013, **23**, 2322-2328.

22 (a) A.-H. Lu, J.-J. Nitz, M. Comotti, C. Weidenthaler, K. Schlichte, C. W. Lehmann, O. Terasaki, F. Schüth, *J. Am. Chem. Soc.*, 2010, **132**, 14152-14162; (b) F. de Clippel, M. Dusselier, R. Van Rompaey, P. Vanelderen, J. Dijkmans, E. Makshina, L. Giebeler, S. Oswald, G. V. Baron, J. F. M. De-nayer, P. P. Pescarmona, P. A. Jacobs, B. F. Sels, *J. Am. Chem. Soc.*, 2012, **134**, 10089-10101.

23 H. Yang, B. Yuan, X. Zhang, *Acc. Chem. Res.*, 2014, **47**, 2106-2115.

24 (a) L. Zhao, T. Ma, H. Bai, G. Lu, C. Li, G. Shi, *Langmuir*, 2008, **24**, 4380-4387; (b) K. Masuda, Y. Ikeda, M. Ogawa, H. Benten, H. Ohkita, S. Ito, *ACS Appl. Mater. Interfaces*, 2010, **2**, 236-245; (c) K. Y. K. Man, H. L. Wong, W. K. Chan, *Langmuir*, 2006, **22**, 3368-3375; (d) J. K. Mwaura, M. R. Pinto, D. Witker, N. Ananthakrishnan, K. S. Schanze, J. R. Reynolds, *Langmuir*, 2005, **21**, 10119-10126; (e) C. W. Tse, K. Y. K. Man, K. W. Cheng, C. S. K. Mak, W. K. Chan, C. T. Yip, Z. T. Liu, A. B. Djurišić, *Chem. Eur. J.*, 2007, **13**, 328-335; (f) C. Luo, D. M. Guldi, M. Maggini, E. Menna, S. Mondini, N. A. Kotov, M. Prato, *Angew. Chem. Int. Ed.*, 2000, **39**, 3905-3909.

25 N. Yaacobi-Gross, N. Garphunkin, O. Solomeshch, A. Vaneski, A. S. Susha, A. L. Rogach, N. Tessler, *ACS nano*, 2012, **6**, 3128-3133.

26 M. Chen, L. Shao, S. V. Kershaw, H. Yu, J. Wang, A. L. Rogach, N. Zhao, *ACS Nano*, 2014, **8**, 8208-8216.

27 B. Cui, Z. Mao, Y. Chen, Y.-W. Zhong, G. Yu, C. Zhan, J. Yao, *Chem. Sci.*, 2015, **6**, 1308-1315.

28 Z. Yang, J. Deng, H. Sun, J. Ren, S. Pan, H. Peng, *Adv. Mater.*, 2014, **26**, 7038-7042.

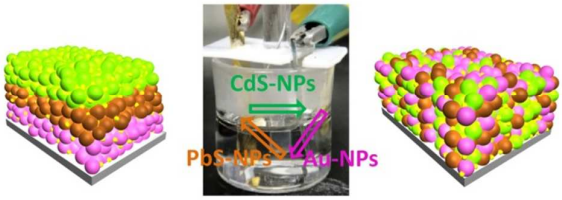

The multiple uniform nanoparticles are electrochemically integrated into thin bulk-hybrid gradient or periodic tandem multilayer films for photovoltaic devices.